Domain Registration in Raft-Mimicking Lipid Mixtures Studied Using Polymer-Tethered Lipid Bilayers

Sumit Garg,* Jürgen Rühe,[†] Karin Lüdtke,[‡] Rainer Jordan,[‡] and Christoph A. Naumann*

*Department of Chemistry and Chemical Biology, Indiana University-Purdue University, Indianapolis, Indiana; [†]Institut für Mikrosystemtechnik, Universität Freiburg, Freiburg, Germany; and [‡]Lehrstuhl für Makromolekulare Stoffe, Department Chemie, Technische Universität München, Munich, Germany

ABSTRACT   The degree of domain registration in a liquid-ordered/liquid-disordered phase-separating lipid mixture consisting of 1-stearoyl-2-oleoyl-sn-3-phosphocholine, egg sphingomyelin, and cholesterol (molar mixing ratio of 1:1:1) was studied using three different planar lipid bilayer architectures distinguished by their bilayer-substrate distance d using epifluorescence microscopy. The bilayer systems, which were built layer by layer using Langmuir-Blodgett/Schaefer film depositions, included a solid-supported bilayer ($d \sim 15$ Å) and two polymer-supported bilayers with $d \sim 30$ Å and $d \sim 58$ Å, respectively. Complete domain registration between Langmuir-Blodgett and Schaefer monolayer domains was observed for $d \sim 58$ Å but not in the cases when $d \sim 15$ Å and $d \sim 30$ Å. Building the bilayer layer by layer guaranteed that any preexisting domains were not in registration initially; our data show that the domain registration observed was not caused by lipid flip-flop or by lateral rearrangement of preexisting large-scale domains. Instead, additional studies on bilayer systems with asymmetric lipid composition indicate that preexisting domains in the Langmuir-Blodgett monolayer induce the formation of completely registered domains in the opposite Schaefer monolayer. This study provides insight into possible biophysical mechanisms of transbilayer domain coupling. Our findings support the concept that the formation of transbilayer signaling platforms based on registered raft domains may occur without the active involvement of membrane-spanning proteins.

INTRODUCTION

Liquid-ordered domains enriched in sphingolipids and cholesterol (CHOL), known as lipid rafts, have received widespread attention from the cell biology and membrane biophysics communities during the last decade because they are believed to play a key role in several important cellular functions, including membrane sorting and trafficking, signal transduction, and cell polarization (1–6). In addition, the pathogenesis of several diseases has been linked to the existence of raft domains (7). Lipid rafts are thought to be associated with both leaflets of the plasma membrane, even though inner and outer leaflet domains may vary in size and composition. It has been suggested that the coupling of inner and outer leaflet rafts may play an important role in signal transduction processes across the plasma membrane (8,9). This concept is supported by the observation that the clustering of glycosylphosphatidylinositol (GPI)-anchored proteins in the outer monolayer leads to coclustering of sarcoma (src)-kinase signaling molecules on the cytosolic side of the plasma membrane and that both types of proteins are part of the detergent-resistant fraction following cold detergent extraction procedures (10). Two different mechanisms of raft-mediated signal transduction have been discussed (9). In the first mechanism, the intermonolayer raft domain coupling is mediated by transmembrane proteins showing raft affinity. In the second mechanism, the raft domain coupling occurs through lateral rearrangements and subsequent over-lapping of outer leaflet rafts containing GPI-anchored proteins and inner leaflet rafts containing src-kinases. The second mechanism does not require the direct involvement of transmembrane proteins. Whereas the first mechanism mainly requires the presence of transmembrane proteins to recruit raft domains, the second one builds on the biophysically driven overlap of liquid-ordered domains, which are phase-separated from the liquid-disordered membrane regions.

Since raft domains are difficult to detect at the cellular level, the topic of domain coupling across the bilayer has been addressed using experiments on model membranes, such as giant unilamellar vesicles (GUVs) and planar solid-supported phospholipid bilayers, exhibiting liquid-ordered/liquid-disordered phase separations. The domains of these model membranes are much easier to detect due to their (typically) larger sizes (11–17). GUVs exhibit the vesicular architecture of a freestanding bilayer of almost symmetric composition. Planar solid-supported phospholipid bilayers, on the other hand, can be assembled layer by layer, thus allowing the formation of asymmetric lipid compositions and leaflet-specific labeling. Fluorescence-based imaging experiments on GUV systems consisting of ternary mixtures of sphingomyelin (SM), CHOL, and phospholipids with partially unsaturated acyl chains have been reported, which exhibit pronounced phase separations between the liquid-ordered and liquid-disordered states (13–15). In these studies, the large-scale domains were found to span through both monolayers, thereby being in complete registration. In contrast, corresponding experiments on comparable lipid mixtures using planar solid-supported bilayers, which are

characterized by a gap between bilayer and solid substrate of only 10–15 Å, exhibit immobilized domains that lack any registration between the two leaflets of the bilayer (16,17). Because liquid-ordered domains in GUVs are registered and those in solid-supported bilayers are immobilized and non-registered, the model membrane studies described above have been very limited in their ability to explore the biophysical mechanisms of raft domain coupling.

Herein we report an epifluorescence microscopy study that provides for the first time to our knowledge insight into the mechanisms of domain registration in raft-mimicking bilayer mixtures. Our study shows that complete registration between domains in both leaflets of the bilayer can be achieved on a planar bilayer architecture built layer by layer using Langmuir-Blodgett/Schaefer (LB/LS) depositions where preexisting domains in the LB and LS monolayers are not in registration immediately upon formation of the bilayer. This is accomplished by lifting the bilayer up sufficiently from the solid substrate via a hydrophilic polymer cushion. In our experimental approach, three different planar bilayer systems of comparable lipid composition (1-stearoyl-2-oleoyl-sn-glycero-3-phosphocholine (SOPC), egg SM, and CHOL (molar mixing ratio of 1:1:1)) but different bilayer-substrate distances d are investigated. The three systems consist of a solid-supported bilayer ($d \sim 17$ Å) and two polymer-tethered bilayers of different polymer layer thicknesses of $d \sim 30$ Å and $d \sim 58$ Å, respectively. For a bilayer system characterized by $d \sim 58$ Å, our results show that preexisting domains in the LB monolayer seem to promote the formation of completely registered domains in the opposite LS monolayer. Furthermore, our data suggest that domain registration does not occur via flip-flop of individual phospholipids and/or via lateral reorganization of large-scale domains in both leaflets of the bilayer. Instead, as additional experiments on asymmetric bilayers indicated, registered domains can be induced across the bilayer. Importantly, this study supports the concept of transbilayer signaling platforms based on registered raft domains after lateral rearrangements of lipid raft domains, as proposed recently (9).

MATERIALS AND METHODS

All nonlabeled membrane constituents, SOPC, 1,2-dioleoyl-sn-glycero-3-phosphocholine (DOPC), 1,2-dipalmitoyl-sn-glycero-3-phosphocholine (DPPC), CHOL, and egg SM, were purchased from Avanti Polar Lipids (Alabaster, AL). The labeled phospholipids N-(7-nitrobenz-2-oxa-1,3-diazol-4-yl)-1,2-dihexadecanoyl-sn-glycero-3-phosphoethanolamine, triethylammonium salt (NBD-DPPE) was obtained from Avanti Polar Lipids, and N-(6-tetrame-

thylrhodaminethiocarbamoyl)-1,2-dihexadecanoyl-sn-glycero-3-phosphoeth-anolamine, triethylammonium salt (TRITC-DPPE) and 1,1'-dioctadecyl-3,3,3',3'-tetramethylindocarbocyanine perchlorate (DiIC$_{18}$) were purchased from Invitrogen/Molecular Probes (Eugene, OR). The lipopolymers dioctadecylamine [poly(2-ethyl-2-oxazoline) 8988] (DODA-E$_{85}$) and dioctadecylamine [poly(2-ethyl-2-oxazoline) 4032] (DODA-E$_{35}$) were synthesized, as described previously (18). The synthesis of dioctadecyl [poly(2-methyl-2-oxazoline)] (DiC$_{18}$-M$_{50}$) is reported elsewhere (19–21). All other chemicals were purchased from Fisher (Fair Lawn, NJ).

Solid-supported and polymer-tethered phospholipid bilayers, which are shown in Fig. 1, were built using procedures described previously (22). Glass coverslips (dimension 24 × 40 mm) were cleaned by baking them at 515°C in a kiln for 3 h, followed by subsequent sonication in three different cleaning solutions of 1% sodium dodecyl sulfate, methanol saturated with NaOH, and 0.1% HCl for 30 min each. After each cleaning solution step, slides were rinsed extensively with Milli-Q water (pH = 5.5, 18 MΩ-cm resistivity). Clean glass slides were stored in Milli-Q and used within 1 week. Lipid mixtures for individual monolayers were prepared by dissolving appropriate molar concentrations of monolayer constituents in chloroform (high-performance liquid chromatography grade). Bilayer architectures were built layer by layer via successive LB and LS monolayer transfer steps using an LB trough (Labcon, Darlington, UK) system, equipped with dipper and computer feedback to control the surface pressure and dipping speed during LB transfer (22). Before transfer of each monolayer, chloroform solutions of corresponding lipid mixtures were spread on the air-water interface followed by the compression of amphiphiles to 30 mN/m and a sufficient equilibration period (typically ~20 min) to guarantee a stable film pressure. The dipper speed during LB transfer was set to 400 μm/s.

Three types of bilayer systems characterized by different bilayer-substrate distances were studied (TYPEs I–III in Fig. 1). The three bilayer types are typically characterized by the same LS monolayer composition of SOPC/SM/CHOL (1:1:1). The LB composition of the TYPE I bilayer consists of SOPC/SM/CHOL (1:1:1) with 5 mol % of lipopolymers added to this lipid mixture to build bilayer systems of TYPEs II and III (lipopolymer (TYPE II): DODA-E$_{35}$; lipopolymer (TYPE III): DODA-E$_{85}$ or DiC$_{18}$-M$_{50}$]. The low lipopolymer molar concentration of 5 mol % was chosen to reduce possible perturbation in the large-scale phase behavior with respect to the lipopolymer-free case. In addition, two asymmetric bilayer systems of TYPE III were studied: I), LB: DOPC/SM/CHOL (1:1:1) + 5 mol % DODA-E$_{85}$, LS: DOPC/SM/CHOL (42:29:29); and II), LB: DOPC/DPPC/CHOL (50:26:24) + 5 mol % DODA-E$_{85}$, LS: DOPC/DPPC/CHOL (66:10:24). In both cases, the asymmetric composition was reversed as well. Finally, one control experiment was conducted on a symmetric bilayer system of TYPE I using a lipid composition of DOPC/SM/CHOL (42:29:29). The experimental conditions and the lipid compositions were chosen to reduce oxidative damage of lipids during the assembly of the bilayer because the LB transfer under argon atmosphere is not feasible. It has been reported that air exposure modifies the film pressure and alters the miscibility transition pressure in monolayers (16).

To visualize coexisting domains, different labeling approaches were pursued. In each case, the dye concentration per monolayer was set to 0.5 mol %. Monolayers were labeled by adding the dye-lipids to the lipid mixtures in chloroform before spreading. In the first labeling approach, both leaflets of the bilayer were labeled using TRITC-DPPE. In the second approach, TRITC-DPPE and NBD-DPPE were added to the LB and LS monolayers, respectively, thus allowing dual color experiments. In another dual color experiment, the monolayers were labeled selectively using NBD-DPPE and
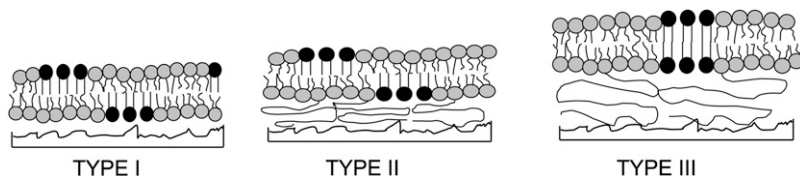

FIGURE 1 Schematic of planar membrane architectures employed, including solid-supported phospholipid bilayer (TYPE I) and polymer-supported phospholipid bilayer based on lipopolymers DODA-E$_{35}$ (TYPE II) and DO-DAE$_{85}$ (TYPE III), respectively. The three bilayer systems are distinguished by different bilayer-substrate distances of ~15 Å (TYPE I), ~30 Å (TYPE II), and ~58 Å (TYPE III).

TYPE I   TYPE II   TYPE III

$DiIC_{18}$. These dye-labeled lipids were chosen because NBD-DPPE tends to partition into liquid-ordered domains, because TRITC-DPPE and $DiIC_{18}$ preferably associate with the liquid-disordered environment, and because $DiIC_{18}$ was shown to be less prone to dye mixing during LS transfer (12,17). Epifluorescence microscopy was conducted using an inverted optical microscope in epiillumination (Axiovert 200M, Zeiss, Oberkochen, Germany) where the beam was focused to the sample by a microscopy objective (Zeiss, water immersion, 40× numerical aperture = 1.2). Images were acquired and analyzed using a CoolSNAPfx charge-coupled device camera (Roper Scientific, Princeton, NJ) and Roper Scientific imaging software.

RESULTS AND DISCUSSION

To explore the relationship between the bilayer-substrate distance and the degree of raft domain registration, the large-scale phase separation that occurs between liquid-ordered and liquid-disordered phase regions was studied on three bilayer systems characterized by similar lipid composition but different bilayer-substrate distances. Recent fluorescence interference microscopy (FLIM) studies have provided bilayer-substrate distances for the solid-supported (TYPE I) and polymer-tethered (comparable to TYPE II) bilayers of $d \sim 17$ Å and $d \sim 39$ Å, respectively (23). There the polymer-tethered bilayer system was built using a low lipopolymer (tethering) molar concentration of 3400-Da poly(ethylene glycol) (PEG) lipopolymers, which is similar to the TYPE II bilayer system studied herein. Interestingly, d obtained for the polymer-tethered phospholipid bilayer system using FLIM agreed well with the calculated Flory radius R_F of the polymer in a coil (mushroom) conformation (23), thus indicating that the polymer conformation of lipopolymers in polymer-tethered bilayers is well characterized by scaling laws of polymer physics (24). If the graft density $\sigma > R_F$ (mushroom conformation), the bilayer-substrate distance d can be approximated in terms of the monomer size a and the number of monomers N per polymer chain via $d \approx R_F = aN^{3/5}$ (good solvent conditions). If $\sigma < R_F$ (brush conformation), d can be written as a function of R_F and σ with $d = R_F(R_F/\sigma)^{2/3}$ (25). The graft density σ can be obtained via $\sigma = 2(A_{poly}/\pi)^{1/2}$, where the area per lipopolymer molecule A_{poly} can be determined from the amount of lipopolymers spread and the total area of the monolayer before LB transfer. Applied to our polymer-tethered bilayer systems, we obtain for TYPE II and III bilayer systems $d = 30$ Å and $d = 58$ Å, respectively. In comparison to a solid-supported bilayer (TYPE I) where $d = 17$ Å, these results illustrate a moderate

lifting up of the bilayer from the solid substrate for TYPE II and a more pronounced one for TYPE III, as illustrated in Fig. 1.

Fig. 2 compares fluorescence micrographs of a ternary mixture of SM/CHOL/SOPC (1:1:1) in a solid-supported phospholipid bilayer (left, TYPE I), and in two polymer-tethered phospholipid bilayers of low concentration of tethered lipids ($c_{tether} = 5$ mol %) distinguished by lipopolymers of different polymer chain lengths, $DODA-E_{35}$ (center, TYPE II) and $DODA-E_{85}$ (right, TYPE III). Here both leaflets of the bilayer are labeled using TRITC-DPPE. The micrographs show that nonoverlapping domains are observed for bilayer systems of TYPEs I and II. In contrast, complete domain registration is found for the TYPE III bilayer system characterized by the largest bilayer-substrate distance. In the latter case, rapid fluorescence recovery of a photobleached area was observed, thus ensuring the formation of the bilayer via its fluidity (not shown). Our findings on solid-supported bilayers (TYPE I) are supported by previous reports of nonregistered domains on comparable bilayer systems (16,17). More importantly, the results presented in Fig. 2 imply that domain registration in a planar model membrane characterized by a liquid-ordered/liquid-disordered phase separation requires the sufficient decoupling of the bilayer from the solid substrate. Furthermore, Fig. 2 shows that the presence of 5 mol % of polymer-tethered lipids in TYPE III bilayers does not prevent the formation of large-scale phase separations. Finally, Fig. 2 indicates that monolayer oxidation does not seem to play a significant role in the formation of registered domains because any potential oxidative damage should be comparable in all three bilayer systems. However, only the TYPE III bilayer system shows registered domains.

Interestingly, the TYPEs I–III bilayers illustrated in Fig. 2 show somewhat different domain shapes. Based on line tension arguments, one would expect that all domains characterized by a liquid-liquid phase separation would relax into a circular shape. In contrast, the inner and outer monolayers of the TYPE I bilayer shown in Fig. 2 typically exhibit almond-shaped and/or elliptical domains. As reported before (16), the almond-shaped domains, which are elongated in the direction of the LB deposition movement across the coverslip, are the result of the LB transfer. Noncircular domains also can be observed for the TYPE II system in Fig. 2. In both cases (TYPEs I and II), the deviation from circular
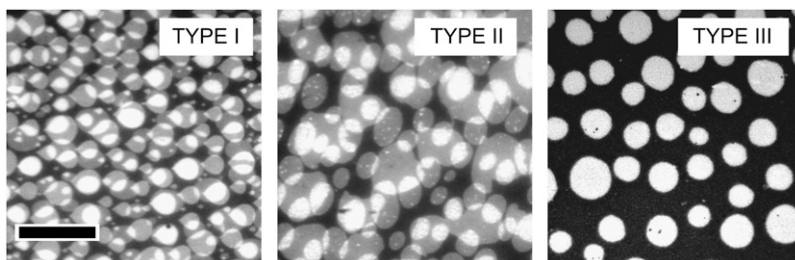

FIGURE 2 Fluorescence micrographs of the ternary mixture SOPC/SM/CHOL (1:1:1) in bilayer systems of TYPE I (*left*), TYPE II (*center*), and TYPE III (*right*). The micrographs illustrate the large-scale liquid-liquid phase separation, which are typical for this mixture. Only the TYPE III bilayer system characterized by the largest bilayer-substrate distance shows domain registration. Both leaflets are labeled using TRITC-DPPE. The scale bar represents 30 μm.

domain geometry suggests epitaxial coupling between glass substrate and bilayer, which prevents the relaxation of domain shapes. Dietrich et al. have envisioned extending glass peaks that act as pinning centers for the fluid-fluid domain boundary (12). Their argument is supported by our finding that a SOPC/SM/CHOL (1:1:1) bilayer on a mica substrate (TYPE I), which is less rough than a glass substrate, results in perfectly circular domains in both of its leaflets without exhibiting domain registration (data not shown). The influence of pinning centers should be reduced if the bilayer-substrate distance is increased. The appearance of increasingly circular domains in DODA-E_{85}-based bilayer systems (TYPE III) seems to confirm this. The additional findings on mica-supported bilayers also indicate that the observed domain registration obtained for TYPE III bilayer systems is more dependent on the bilayer-substrate distance than different degrees of pinning.

To verify the domain registration in TYPE III bilayers, Fig. 3, A–F, shows fluorescence micrographs obtained from polymer-tethered bilayers based on DODA-E_{85} where each monolayer of the bilayer was labeled using a different dye. Two different labeling approaches were employed. In the first approach, the LB and LS monolayers were labeled using TRITC-DPPE and NBD-DPPE, respectively. Fig. 3, A and B, illustrates the same area of the bilayer through the TRITC (Fig. 3 A) and NBD (Fig. 3 B) channels. A comparison of both fluorescence images reveals that domain shapes and positions in both channels exactly match, thus supporting the finding of complete domain registration in TYPE III bilayers as illustrated in Fig. 2. Fig. 3, C and D, shows the recovery of a photobleaching spot, thus verifying the existence of the bilayer through the detection of its fluidity. Recently, it was shown that partial mixing of dye-labeled lipids may occur during LS transfer but that such a mixing was not observed for $DiIC_{18}$ (17). Therefore, to verify further the existence of registered large-scale domains in the LS monolayer of TYPE III bilayers, a second labeling approach was pursued where the LB and LS monolayers were labeled using NBD-DPPE and $DiIC_{18}$, respectively. Fig. 3, E and F, illustrates the corresponding micrographs visualizing the NBD (Fig. 3 E) and DiI (Fig. 3 F) probes. Clearly, large-scale domains can be observed in the LS monolayer, which are in complete registration with their LB counterparts.

It has been reported that large-scale phase separations in solid-supported bilayers might be comparable to those found in Langmuir monolayers at the air-water interface before LB transfer (16). However, the layer-by-layer design of the bilayer systems, as employed herein, excludes the possibility of domains being in registration immediately after the bilayer is completed via LS transfer. Furthermore, it has been shown in solid-supported bilayers containing liquid-gel mixtures that domain rearrangements are mainly caused by lipid flip-flop (26). As a consequence, three possible mechanisms to induce the observed domain registration in TYPE III membranes need to be considered: 1), lateral rearrangements of
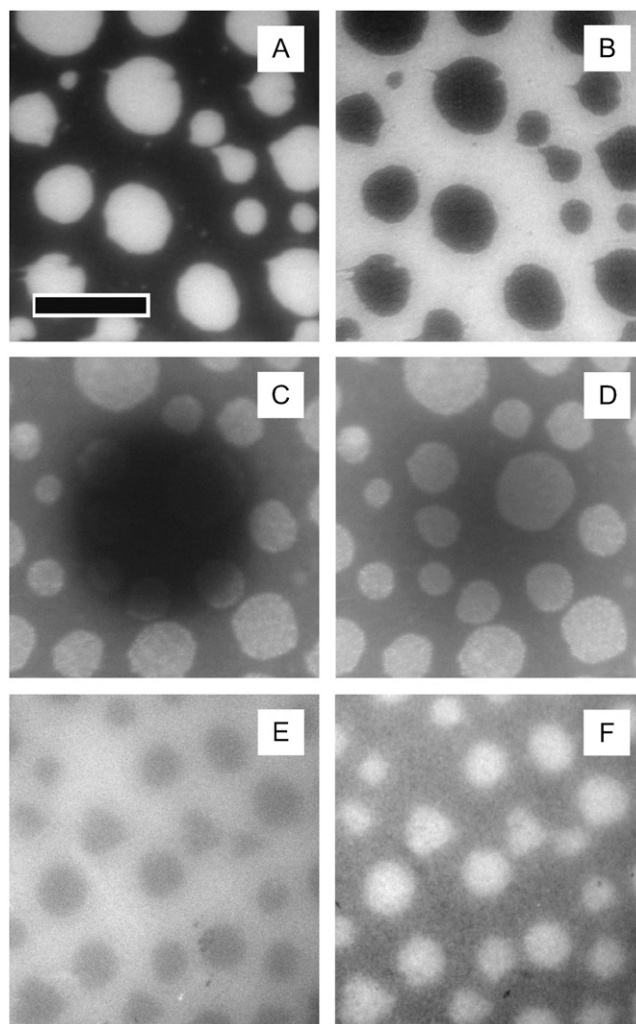

FIGURE 3 Fluorescence micrographs obtained from dual-color labeling experiments on a TYPE III bilayer system using two different labeling procedures. In the first procedure, the inner leaflet is labeled using TRITC-DPPE, which preferably associates with liquid-disordered regions of the bilayer, the outer one is labeled using NBD-DPPE with affinity for liquid-ordered regions. Fluorescence micrographs of the bilayer are depicted, as observed through the TRITC (A) and NBD (B) channels. Fluorescence recovery after photobleaching data (C and D) show fast fluorescence recovery, thus verifying the existence of the fluid bilayer. E and F illustrate micrographs obtained using a second labeling procedure. Here the LB and LS monolayers are labeled using NBD-DPPE and DiIC18, respectively, and imaged through the NBD (E) and DiIC18 (F) channels. The scale bar represents 30 μm.

preexisting large-scale domains; 2), lipid flip-flop-based processes; and 3), phase separations induced by preexisting large-scale domains in the opposite monolayer. These three mechanisms will be discussed separately below.

In the first proposed mechanism, the LS monolayer contains preexisting large-scale domains which are completely distinct from the LB monolayer but which quickly rearrange laterally to become registered with their LB counterparts. Kaizuka and Groves recently showed on supported intermembrane junctions that the lateral diffusion of domains in a planar bilayer can be estimated by considering the lateral

diffusion of a disk in a two-dimensional fluid, which can be expressed via the Einstein relation

$$D = \frac{kT}{\lambda}, \qquad (1)$$

where k is the Boltzmann constant, T is the temperature, and λ represents the drag coefficient (27). In case of frictional coupling between a bilayer and a nearby solid substrate, λ can be described by (28,29)

$$\lambda = 4\pi\eta_m z_m \left(\frac{\varepsilon^2}{2} + \frac{\varepsilon K_1(\varepsilon)}{K_0(\varepsilon)} \right) \qquad (2)$$

with

$$\varepsilon \approx a \left(\frac{\alpha\eta_w}{\eta_m z_m d} \right)^{1/2}. \qquad (3)$$

Here η_m and z_m are the viscosity and thickness of the membrane, K_0 and K_1 are modified Bessel functions of the second kind, ε is the nondimensional radius, a is the radius of the disk, α is a constant, η_w is the viscosity of water, and d is the thickness between the bilayer and the substrate. With an average domain size of ~ 10 μm and a bilayer-substrate distance of $d = 58$ Å, Eqs. 1–3 provide a lateral diffusion coefficient of $D \sim 10^{-4}$ μm^2/s. This diffusion coefficient is several orders of magnitude smaller than necessary to facilitate the diffusion-based rearrangement over a distance of ~ 7 μm, corresponding to half the average distance between neighboring domains within 10 min (duration between completion of bilayer and imaging). Furthermore, no measurable lateral mobility of large-scale domains (registered and nonregistered) could be detected in bilayers of TYPEs I–III over a time period of 48 h (data not shown), thus indicating the immobilization of large-scale domains. Therefore, the lateral rearrangement of large-scale domains is not a plausible mechanism of domain registration in TYPE III bilayers. It should be noted, however, that lateral rearrangements of individual lipids and small lipid clusters do occur in the liquid-liquid phase-separations studied.

Second, to address the question of whether domain registration is induced by flip-flop, Fig. 4, *A* and *B*, shows fluorescence micrographs where the same membrane region of a TYPE III bilayer is imaged before (Fig. 4 *A*) and after (Fig. 4 *B*) completion of the bilayer. In this case, the bilayer system was built by replacing DODA-E$_{85}$ with DiC$_{18}$-M$_{50}$. Again the completion of the bilayer was verified by evaluating the fluorescence recovery after photobleaching (data not shown). A visual comparison of Fig. 4, *A* and *B*, shows that the pattern of large-size domains in the LB and LB/LS systems is almost identical. Only a few small domains visible in the LB monolayer seem to have disappeared in the LB/LS system. Importantly, these findings exclude transbilayer lipid flip-flop as the major molecular mechanism for the formation of registered domains in TYPE III bilayers because such a mechanism would result in a decrease of the average domain
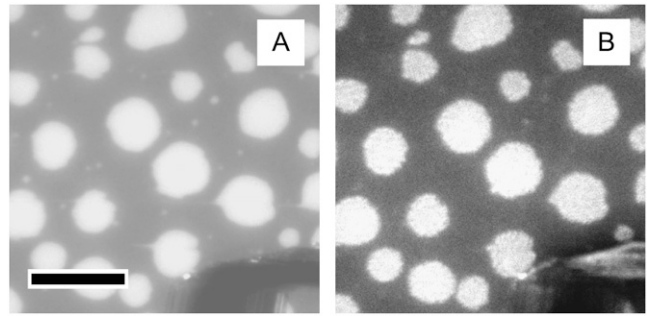

FIGURE 4 Fluorescence micrographs of TYPE III bilayer systems comparing the large-scale phase separations of the same membrane region on the monolayer after LB-transfer (*A*) and the bilayer after LB/LS transfers. The scratch at bottom right of each micrograph was added to guarantee that the same membrane region is compared. The scale bar represents 30 μm.

size in the LB/LS system relative to its LB counterpart, but this was not observed. Furthermore, large-scale phase separations indicating nonregistered domains in bilayers of TYPEs I and II remained unchanged over several days.

The latter findings are different than results using liquid-gel phase separating bilayers of TYPE I formed via vesicle fusion reported by Longo and co-workers (26). They found that registered gel domains are stable over time but that nonregistered ones change their size and shape, apparently due to flip-flop. Most likely, this discrepancy can be explained by the fact that their study was performed on bilayers containing liquid-gel phase separations (without CHOL and SM), whereas the data presented herein focus on bilayers characterized by liquid-ordered/liquid-disordered phase separations. Fig. 4, *A* and *B*, shows that domains in the LB monolayer of a TYPE III bilayer system are immobilized. Fig. 4, *A* and *B*, also indicates that if nonregistered domains had formed in the LS monolayer of TYPE III systems on completion of the bilayer, which is not unreasonable under our experimental conditions, they must have dissolved quickly since the LS monolayer only contains registered domains. In contrast, TYPE I and II bilayers exhibited immobilized nonregistered domains in the LS monolayer (Fig. 2, *A* and *B*), which may have been transferred from the air-water interface. Finally, Fig. 4, *A* and *B*, shows that the phenomenon of domain registration is not limited to TYPE III bilayers built using DODA-E$_{85}$.

The above findings suggest that the registered domains in the LS layer are induced by preexisting large-scale domains in the opposite (LB) monolayer. To verify this mechanism, experiments have been conducted using two different asymmetric bilayer systems. The first asymmetric bilayer system is characterized by compositions with different domain contrasts. Here the composition of the LB monolayer is kept as before (lipid mixture: DOPC/SM/CHOL (1:1:1) + 5 mol % DODA-E$_{85}$), but the composition of the LS monolayer is modified to DOPC/SM/CHOL (42:29:29). The different phase contrasts are illustrated in Fig. 5, *A* and *C*, where
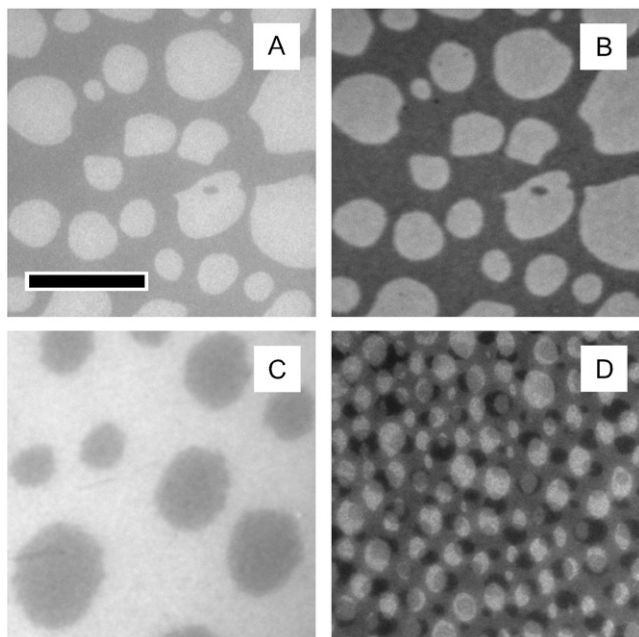
FIGURE 5 Fluorescence micrographs showing the same region of the membrane before (*A*) and after (*B*) LS transfer. LB and LS layers are characterized by different compositions; LB: SOPC/SM/CHOL (1:1:1) +5 mol % DODA-E$_{85}$ and LS: SOPC/SM/CHOL (42:29:29). *C* shows the fluorescence micrograph of an LB monolayer consisting of SOPC/SM/CHOL (42:29:29). *D* illustrates the micrograph obtained using a composition, where the LB and LS compositions are reversed. LB and LS monolayers are labeled using TRITC-DPPE. The scale bar represents 30 μm.

epifluorescence micrographs of LB monolayers of both compositions are compared. Whereas DOPC/SM/CHOL (1:1:1) + 5 mol % DODA-E$_{85}$ is characterized by bright domains embedded in a dark connecting phase (Fig. 5 *A*), DOPC/SM/CHOL (42:29:29) shows dark domains embedded in a bright connecting phase (label TRITC-DPPE). Identical contrasts can be observed if the same compositions are studied in symmetric bilayers (data not shown). Fig. 5, *A* and *B*, presents epifluorescence micrographs from the same region of the LB monolayer (Fig. 5 *A*) and the completed LB/LS bilayer (Fig. 5 *B*) of the first asymmetric bilayer system. Interestingly, complete domain registration can be observed in the bilayer despite the different lipid compositions. Furthermore, the LS lipid composition (DOPC/SM/CHOL (42:29:29)) has adapted the same phase contrast as the opposite LB monolayer, thus indicating the LB-induced formation of registered domains in the LS layer. Fig. 5 *D* also shows a micrograph from a TYPE III bilayer, where the bilayer asymmetry was reversed relative to Fig. 5, *A* and *B*. Surprisingly, no registration is observed in this case and both monolayers show opposite domain contrasts, as one might expect for the lipid compositions employed. The latter result is of importance because it verifies that an asymmetric bilayer composition is maintained after LS transfer. Recently, it has been reported that the bilayer asymmetry may be reduced due to lipid mixing during LB/LS bilayer formation (31).

To go one step further and to ask whether registered domains can be induced in monolayers which typically do not show any large-scale phase separation, the second asymmetric bilayer system of TYPE III is based on LB and LS monolayer compositions, which are separated by a phase boundary (LB: DOPC/DPPC/CHOL (50:26:24) + 5 mol % DODA-E$_{85}$, LS: DOPC/DPPC/CHOL (66:10:24)). Interestingly, this phase boundary seems to coincide with a phase boundary reported for DOPC/DPPC/CHOL mixed bilayers in a GUV architecture (14), even though it has been reported that the phase behavior in monolayer and bilayer systems can be quite different (30). Fig. 6 illustrates the fluorescence micrographs obtained from such an asymmetric bilayer system. Remarkably, domains in the LB monolayer (Fig. 6 *A*) induce registered domains in the opposite monolayer containing a nonphase separating lipid composition (Fig. 6 *B*). Notably, registration can be observed even though the CHOL molar concentration in the LB and LS monolayer is comparable. The latter point is relevant because CHOL has the ability to adapt to LB-monolayer-induced changes in the LS layer by rapid equilibration in plane of the monolayer or across (flipping). Such mechanisms may be particularly important if the initial LB and LS compositions are characterized by a CHOL gradient, as employed in the asymmetric bilayer system presented in Fig. 5. Fig. 6, *C* and *D*, shows the corresponding results after reversing the compositions. In
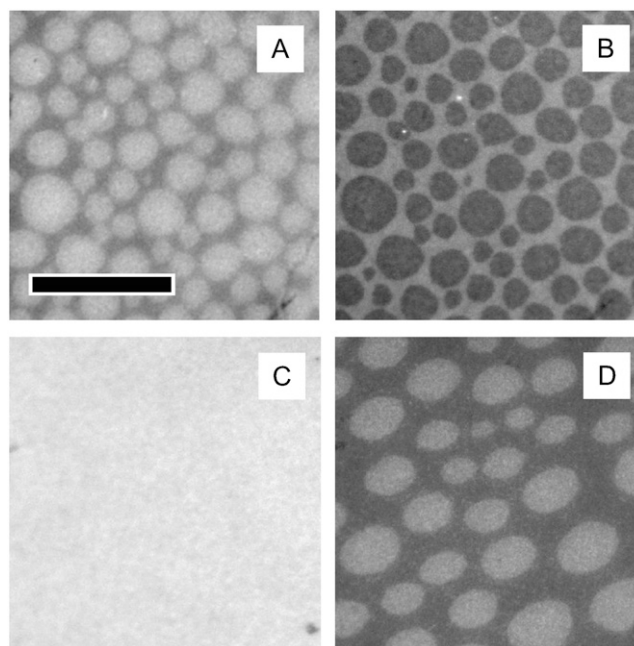

FIGURE 6 Fluorescence micrographs of another asymmetric bilayers system of TYPE III; LB: DOPC/DPPC/CHOL (50:26:24) +5 mol % DODA-E$_{85}$ and LS: DOPC/DPPC/CHOL (66:10:24). LB and LS monolayers are labeled using NBD-DPPE and DiIC$_{18}$, respectively. The bilayer is shown through the NBD (*A*) and DiIC$_{18}$ (*B*) channels. *C* and *D* illustrate corresponding micrographs of the LB and LS layers of a TYPE III bilayer of reversed composition. In this case, LB and LS monolayers are labeled using DiIC$_{18}$ and NBD-DPPE, respectively. The scale bar represents 30 μm.

this case, domains in the LS layer can form even though no phase separation is found in its LB counterpart. This result also suggests that liquid-disordered regions within the LB monolayer cannot induce disorder among ordered lipids across the bilayer.

A comparison between results obtained from both asymmetric bilayer systems reveals several interesting results. Preexisting domains in the LB monolayer have the ability to induce registered domains in the LS monolayer, even if the composition of the latter does not show any domain formation in a symmetric bilayer. In addition, domain registration can be observed independent of the domain contrast in the LB monolayer (liquid-ordered domains in liquid-disordered connecting phase versus liquid-disordered domains in a liquid-ordered connecting phase). Finally, simple reversion of compositions in both asymmetric bilayer systems does not cause the LS monolayer to adapt the phase properties of the LB monolayer. Interestingly, the common theme in both asymmetric bilayers studied is that registration does occur if the LS monolayer contains a higher concentration of unsaturated phospholipids than the LB monolayer. Nevertheless, the interpretation of failed registration due to compositional reversion is rather complicated. This is because of the asymmetric nature of the model membranes employed. First, as our study shows, domain structures in the LB monolayer are pinned to the substrate, whereas the LS monolayer has the ability to adapt its phase properties to domain properties in the LB monolayer. Second, the LB monolayer is more ordered than its LS counterpart due to its closer vicinity to the solid substrate (32) and because of the potential ability of membrane-associated polymers to order lipids in the LB monolayer. We also should point out that our findings in symmetric bilayers of TYPE III show that registered domains can form if the concentration of unsaturated lipids in both monolayers is comparable.

The results above support a mechanism of domain registration where domains in the LB monolayer induce the formation of registered domains in the LS one. Our findings imply that the transbilayer interaction is comparably strong relative to the mixing energies within the LS monolayer. To understand how registered domains are stabilized, concepts of intermonolayer coupling should be considered. Traditionally, intermonolayer coupling has been discussed based on the geometry and flexibility of the bilayer expressed by a local bilayer asymmetry and curvature and by local density differences between both leaflets of the bilayer (33–39). In addition, direct interleaflet van der Waals interactions may play a significant role in intermonolayer coupling (40,41). Such van der Waals interactions depend on the chain-conformational states and the spatial packing of the interacting molecules in both monolayers. Based on this concept of intermonolayer coupling, the stabilization of registered raft domains appears to be plausible because liquid-ordered (raft) and liquid-disordered membrane environments exhibit different lateral densities. Based on similar arguments, the observed registration of gel-phase domains in GUVs has been interpreted in terms of stronger intermonolayer acyl chain interactions of gel domains versus fluid ones (11).

CONCLUSION

This study shows for the first time to our knowledge that complete intermonolayer domain registration can be observed on a planar bilayer system built layer by layer using LB/LS transfers. The domain registration was achieved by decoupling the bilayer from the underlying substrate via a sufficiently thick hydrophilic polymer layer. The data presented herein indicate that the observed domain registration is not caused by lipid flip-flop or lateral rearrangements of large-scale domains in both leaflets of the bilayer. Instead, our experimental results obtained from asymmetric bilayer systems support a mechanism where preexisting domains in the LB monolayer of the bilayer induce phase separations in the opposite (LS) monolayer. Because our study was conducted on raft-mimicking lipid mixtures, the results could be relevant to an understanding of the biophysical mechanisms of transbilayer raft domain formation facilitating raft-mediated transbilayer signaling. It has been argued that only stable raft domains, which are formed after clustering of small, transient rafts via cross-linking of raft-associated proteins (42–44), show signaling capabilities (9). Our findings support the concept that stable raft domains in the outer monolayer of the cell membrane have the ability to recruit small liquid-ordered domains in the inner one to form a transbilayer raft region, even though the latter is less prone to domain formations. Importantly, because this study was conducted without membrane proteins, our data do not exclude the possibility that transbilayer raft domains can be formed without the active participation of membrane-spanning proteins, as proposed previously (9). After completion of the review process, we became aware of a complementary study by Tamm and co-workers, which is based on raft-mimicking lipid mixtures in polymer-tethered bilayers formed via LB transfer and vesicle fusion (45). Interestingly, this group reported that coupling of liquid-ordered domains could be observed if the lipid composition of the top monolayer was composed of complex inner leaflet mixtures containing phosphatidylethanolamine and phosphatidylserine, but not if phosphatidylcholine-CHOL mixtures were used instead. Based on this result, the authors proposed that the formation of registered domains may require the existence of complex lipid compositions. Our study shows, however, that registered domains can form in less complex mixtures as well, thus suggesting a more general mechanism of transbilayer domain coupling.

REFERENCES

1. Simons, K., and E. Ikonen. 1997. Functional rafts in cell membranes. *Nature.* 387:569–572.

2. Janes, P. W., S. C. Ley, A. I. Magee, and P. S. Kabouridis. 2000. The role of lipid rafts in T cell antigen receptor (TCR) signaling. *Semin. Immunol.* 12:23–34.

3. Cherukuri, A., M. Dykstra, and S. K. Pierce. 2001. Floating the raft hypothesis: lipid rafts play a role in immune cell activation. *Immunity.* 14:657–660.

4. Simons, K., and G. van Meer. 1988. Lipid sorting in epithelial cells. *Biochemistry.* 27:6197–6202.

5. Bretscher, M. S., and S. Munro. 1993. Cholesterol and the Golgi apparatus. *Science.* 261:1280–1281.

6. Simons, K., and R. Ehehalt. 2002. Cholesterol, lipid rafts, and disease. *J. Clin. Invest.* 110:597–603.

7. Pierini, L. M., R. J. Eddy, M. Fuortes, S. Seveau, C. Casulo, and F. R. Maxfield. 2003. Membrane lipid organization is critical for human neutrophil polarization. *J. Biol. Chem.* 278:10831–10841.

8. Simons, K., and D. Toomre. 2000. Lipid rafts and signal transduction. *Nat. Rev. Mol. Cell Biol.* 1:31–39.

9. Kusumi, A., I. Koyama-Honda, and K. Suzuki. 2004. Molecular dynamics and interactions for creation of stimulation-induced stabilized rafts from small unstable steady-state rafts. *Traffic.* 5:213–230.

10. Stefanova, I., V. Horejsi, I. J. Ansotegui, W. Knapp, and H. Stockinger. 1991. GPI-anchored cell-surface molecules complexed to protein tyrosine kinases. *Science.* 254:1016–1019.

11. Bagatolli, L. A., and E. Gratton. 2000. Two photon fluorescence microscopy of coexisting lipid domains in giant unilamellar vesicles of binary phospholipid mixtures. *Biophys. J.* 78:290–305.

12. Dietrich, C., L. A. Bagatolli, Z. N. Volovyk, N. L. Thompson, M. Levi, K. Jacobson, and E. Gratton. 2001. Lipid rafts reconstituted in model membranes. *Biophys. J.* 80:1417–1428.

13. Bagatolli, L. A. 2003. Direct observation of lipid domains in free standing bilayers: from simple to complex lipid mixtures. *Chem. Phys. Lipids.* 122:137–145.

14. Veatch, S. L., and S. L. Keller. 2003. Separation of liquid phases in giant vesicles of ternary mixtures of phospholipids and cholesterol. *Biophys. J.* 85:3074–3083.

15. Veatch, S. L., I. V. Polozov, K. Gawrisch, and S. L. Keller. 2004. Liquid domains in vesicles investigated by NMR and fluorescence microscopy. *Biophys. J.* 86:2910–2922.

16. Stottrup, B. L., S. L. Veatch, and S. L. Keller. 2004. Nonequilibrium behavior in supported lipid membranes containing cholesterol. *Biophys. J.* 86:2942–2950.

17. Crane, J. M., and L. K. Tamm. 2004. Role of cholesterol in the formation and nature of lipid rafts in planar and spherical model membranes. *Biophys. J.* 86:2965–2979.

18. Lehmann, T. 1999. Synthese von kovalent an Oberflächen fixierten Polyethyloxazolinfilmen zum Aufbau polymergestützter Biomembran-Modelle. PhD thesis. Johannes Gutenberg-Universität Mainz, Mainz, Germany.

19. Jordan, R., H. Martin, K. Raeder, and K. K. Unger. 2001. Lipopolymers for surface functionalizations: 1. Synthesis and characterization of terminal functionalized poly(*N*-propionylethylenimine)s. *Macromolecules.* 34:8858–8865.

20. Purrucker, O., A. Förtig, R. Jordan, and M. Tanaka. 2004. Supported membranes with well-defined polymer tethers—incorporation of cell receptors. *ChemPhysChem.* 5:327–335.

21. Purrucker, O., A. Förtig, K. Lüdtke, R. Jordan, and M. Tanaka. 2005. Confinement of transmembrane cell receptors in tunable stripe micropatterns. *J. Am. Chem. Soc.* 127:1258–1264.

22. Deverall, M. A., E. Gindl, E.-K. Sinner, H. Besir, J. Ruehe, M. J. Saxton, and C. A. Naumann. 2005. Membrane lateral mobility obstructed by polymer-tethered lipids studied at the single molecule level. *Biophys. J.* 88:1875–1886.

23. Kiessling, V., and L. K. Tamm. 2003. Measuring distances in supported bilayers by fluorescence interference-contrast microscopy: polymer supports and SNARE proteins. *Biophys. J.* 84:408–418.

24. de Gennes, P. G. 1987. Polymers at an interface: a simplified view. *Adv. Colloid Interface Sci.* 27:189–209.

25. Jones, R. A. L., and R. W. Richards. 1999. Polymers at Surfaces and Interfaces. Cambridge University Press, Cambridge, UK.

26. Lin, W.-C., C. D. Blanchette, T. Ratto, and M. J. Longo. 2006. Lipid asymmetry in DLPC/DSPC-supported lipid bilayers: a combined AFM and fluorescence microscopy study. *Biophys. J.* 90:228–237.

27. Kaizuka, Y., and J. T. Groves. 2004. Structure and dynamics of supported intermembrane junctions. *Biophys. J.* 86:905–912.

28. Evans, E., and E. Sackmann. 1988. Translational and rotational drag coefficients for a disk moving in a liquid membrane associated with a rigid substrate. *J. Fluid Mech.* 194:553–561.

29. Merkel, R., E. Sackmann, and E. Evans. 1989. Molecular friction and epitactic coupling between monolayers in supported bilayers. *J. Phys. France.* 50:1535–1555.

30. Stottrup, B. L., D. S. Stevens, and S. L. Keller. 2005. Miscibility of ternary mixtures of phospholipids and cholesterol in monolayers, and application to bilayer systems. *Biophys. J.* 88:269–276.

31. Crane, J. M., V. Kiessling, and L. K. Tamm. 2005. Measuring lipid asymmetry in planar supported bilayers by fluorescence interference contrast microscopy. *Langmuir.* 21:1377–1388.

32. Hetzer, M., S. Heinz, S. Grage, and T. M. Bayerl. 1998. Asymmetric molecular friction in supported phospholipid bilayers revealed by NMR measurements of lipid diffusion. *Langmuir.* 14:982–984.

33. Leibler, S. 1986. Curvature instability in membranes. *J. Phys. (Paris).* 47:507–516.

34. Safran, S. A., P. Pincus, and D. Andelman. 1990. Theory of spontaneous vesicle formation in surfactant mixtures. *Science.* 248:354–356.

35. Safran, S. A., P. Pincus, D. Andelman, and F. C. McKintosh. 1991. Stability and phase behavior of mixed surfactant vesicles. *Phys. Rev. A.* 43:1071–1078.

36. McKintosh, F. C. 1994. Mixed fluid bilayers: effects of confinement. *Phys. Rev. E. Stat. Phys. Plasmas. Fluids Relat. Interdiscip. Topics.* 50:2891–2897.

37. Seifert, U. 1993. Curvature-induced lateral phase segregation in two-component vesicles. *Phys. Rev. Lett.* 70:1335–1338.

38. Kozlov, M. M., and W. Helfrich. 1992. Effects of a cosurfactant on the stretching and bending elasticities of a surfactant monolayer. *Langmuir.* 8:2792–2797.

39. Helfrich, W., and M. M. Kozlov. 1993. Bending tensions and the bending rigidity of fluid membranes. *J. Phys. II.* 3:287–292.

40. Zhang, Z., M. Zuckerman, and O. L. Mouritsen. 1992. Effect of intermonolayer coupling on phase behavior of lipid bilayers. *Phys. Rev. A.* 46:6707–6713.

41. Hansen, P. L., L. Miao, and J. H. Ipsen. 1998. Fluid lipid bilayers: intermonolayer coupling and its thermodynamic manifestations. *Phys. Rev. E.* 58:2311–2324.

42. Harder, T., P. Scheiffele, P. Verkrade, and K. Simons. 1998. Lipid domain structure of the plasma membrane revealed by patching of membrane components. *J. Cell Biol.* 141:929–942.

43. Harder, T., and K. Simons. 1999. Clusters of glycolipid and glycosylphosphatidylinositol-anchored proteins in lymphoid cells: accumulation of actin regulated by local tyrosine phosphorylation. *Eur. J. Immunol.* 29:556–562.

44. Janes, P. W., S. C. Ley, and A. I. Magee. 1999. Aggregation of lipid rafts accompanies signaling via the T cell antigen receptor. *J. Cell Biol.* 147:447–461.

45. Kiessling, V., J. M. Crane, and L. K. Tamm. 2006. Transbilayer effects of raft-like lipid domains in asymmetric planar bilayers measured by single molecule tracking. *Biophys. J.* 91:3313–3326.